Developmental Biology 394 (2014) 314–326

Contents lists available at ScienceDirect

Developmental Biology

journal homepage: www.elsevier.com/locate/developmentalbiology

Ins-4 and *daf-28* function redundantly to regulate *C. elegans* L1 arrest

Yutao Chen, L. Ryan Baugh*

Department of Biology, Duke Center for Systems Biology, Duke University, Durham, NC 27708, USA

ARTICLE INFO

Article history:
Received 7 March 2014
Received in revised form
8 July 2014
Accepted 4 August 2014
Available online 14 August 2014

Keywords:
L1 arrest
Diapause
Starvation
Caenorhabditis elegans
Insulin

ABSTRACT

Caenorhabditis elegans larvae reversibly arrest development in the first larval stage in response to starvation (L1 arrest or L1 diapause). Insulin-like signaling is a critical regulator of L1 arrest. However, the *C. elegans* genome encodes 40 insulin-like peptides, and it is unknown which peptides participate in nutritional control of L1 development. Work in other contexts has revealed that insulin-like genes can promote development ("agonists") or developmental arrest ("antagonists"), suggesting that such agonists promote L1 development in response to feeding. We measured mRNA expression dynamics with high temporal resolution for all 40 insulin-like genes during entry into and recovery from L1 arrest. Nutrient availability influences expression of the majority of insulin-like genes, with variable dynamics suggesting complex regulation. We identified thirteen candidate agonists and eight candidate antagonists based on expression in response to nutrient availability. We selected ten candidate agonists (*daf-28, ins-3, ins-4, ins-5, ins-6, ins-7, ins-9, ins-26, ins-33* and *ins-35*) for further characterization in L1 stage larvae. We used destabilized reporter genes to determine spatial expression patterns. Expression of candidate agonists is largely overlapping in L1 stage larvae, suggesting a role of the intestine, chemosensory neurons ASI and ASJ, and the interneuron PVT in control of L1 development. Transcriptional regulation of candidate agonists is most significant in the intestine, as if internal nutrient status is a more important influence on transcription than sensory perception. Phenotypic analysis of single and compound deletion mutants did not reveal effects on L1 developmental dynamics, though simultaneous disruption of *ins-4* and *daf-28* increases survival of L1 arrest. Furthermore, overexpression of *ins-4*, *ins-6* or *daf-28* alone decreases survival and promotes cell division during starvation. These results suggest extensive functional overlap among insulin-like genes in nutritional control of L1 development while highlighting the role of *ins-4, daf-28* and to a lesser extent *ins-6*.

Introduction

The nematode *Caenorhabditis elegans* has evolved various developmental responses to survive fluctuations in food supply. Dauer larvae form as an alternative to the third larval stage in response to high population density and limited food (reviewed in Riddle and Albert (1997)). However, dauer larvae must feed to develop. In contrast, larvae that hatch without food respond to starvation by reversibly arresting development in the first larval stage (L1 arrest or L1 diapause) (reviewed in Baugh (2013)). Unlike dauer larvae, arrested L1 larvae have no morphological modification, though stress resistance is increased. Because L1 arrest and recovery are governed by nutrient availability alone, the system provides a powerful model to study nutritional control of development.

Insulin-like signaling is a critical regulator of L1 arrest. Mutation of the insulin-like receptor *daf-2*/InsR causes constitutive L1 arrest and increased starvation resistance (Baugh and Sternberg, 2006; Munoz and Riddle, 2003). In contrast, mutation of a transcription factor antagonized by insulin-like signaling, *daf-16*/FOXO, or a negative regulator of signaling, *daf-18*/PTEN, causes an L1 arrest-defective phenotype and increased starvation sensitivity (Baugh and Sternberg, 2006; Fukuyama et al., 2006). Mutations affecting insulin-like signaling upstream of the receptor also influence L1 arrest and development. Mutation of *asna-1* or *unc-31*/CAPS, both of which promote insulin-like peptide secretion, phenocopy *daf-2*/InsR mutants by causing constitutive L1 arrest and increased starvation resistance, respectively (Kao et al., 2007; Lee and Ashrafi, 2008). However, the insulin-like peptides that regulate L1 arrest have not been identified.

The *C. elegans* genome contains 40 insulin-like genes. Reporter gene analysis revealed expression in a variety of tissues including the nervous system, intestine, epidermis, vulva and pharynx (Pierce et al., 2001). However, this analysis included only fourteen insulin-like genes, and condition-specific expression was not analyzed. We developed a quantitative assay for insulin-like mRNA expression based on the nCounter platform and used it to measure expression in each developmental stage as well as L1 arrest and dauer larvae (Baugh et al., 2011). However, expression dynamics

* Corresponding author.
E-mail address: ryan.baugh@duke.edu (L.R. Baugh).

http://dx.doi.org/10.1016/j.ydbio.2014.08.002

and spatial patterns were not analyzed. More recently, reporter gene analysis was reported for all 40 insulin-like genes throughout development and in different conditions (Ritter et al., 2013). This analysis revealed complex stage- and condition-specific expression patterns. Given these relatively broad characterizations of insulin-like gene expression, expression dynamics and precise cellular patterns have not been reported for a specific developmental process controlled by insulin-like signaling such as L1 arrest and recovery.

Over-expression experiments revealed that individual insulin-like peptides could promote development or arrest, suggesting they function as agonists or antagonists, respectively, of DAF-2/InsR (Pierce et al., 2001). Loss-of-function phenotypes are consistent with the agonist/antagonist distinction, and they provide examples of relatively specific function despite such a large gene family. For example, *daf-28* promotes dauer bypass (Li et al., 2003), *ins-6* promotes dauer recovery (Cornils et al., 2011), *ins-3* and *ins-33* promote germline proliferation (Michaelson et al., 2010) and *ins-7* promotes aging (Murphy et al., 2003), suggesting that the peptides encoded by these genes function as DAF-2 agonists. In contrast, *ins-1*, *ins-17* and *ins-18* promote dauer formation, and *ins-18* also promotes longevity, suggesting that these peptides function as DAF-2 antagonists (Cornils et al., 2011; Hung et al., 2014; Matsunaga et al., 2012a, 2012b). Comprehensive analysis of insulin-like gene function in a variety of contexts supports the view that insulin-like genes have relatively specific functions, and it suggested that the distinction between agonist and antagonist may be context-dependent (Fernandes de Abreu et al., 2014). Nonetheless, the functional role of individual insulin-like genes in L1 arrest and recovery has not been investigated.

We report here a comprehensive analysis of insulin-like gene expression dynamics during entry into and recovery from L1 arrest. We validate the results and determine specific sites of expression using destabilized reporter gene analysis. This analysis identifies candidate agonists and antagonists as well as a limited number of anatomical sites that potentially contribute to systemic control of L1 development. We also report extensive phenotypic analysis of deletion mutants during L1 arrest and recovery, demonstrating redundant regulation by *ins-4* and *daf-28*, with *ins-6* making a less significant contribution. Though our results demonstrate that insulin-like genes act redundantly to regulate L1 development they also highlight a relatively specific role of individual insulin-like genes.

Materials and methods

C. elegans genetics

Alleles used in this research include wild-type (Bristol N2); daf-28(tm2308); ins-3(rb1915); ins-4(tm3620); ins-5(tm2560); ins-6 (tm2416); ins-7(tm2001); ins-9(tm3618); ins-26(tm1983); ins-33 (tm2988); ins-35(ok3297); ins-4, ins-5, ins-6(hpDf761); daf-2 (e1370); daf-16(mgDf50); ayIs7[Phlh-8::GFP]; sma-9(wk55); unc-119(ed4) and him-5(e1490). Different allelic combinations were created using standard genetic techniques. The list of YFP reporter gene strains constructed for expression analysis and primers used can be found in Table S1. The list of transgenic strains constructed for complementation analysis and primers used can be found in Table S2.

RNA preparation and expression analysis

Worm culture, RNA sample collection and nCounter analysis were performed as previously described (Baugh et al., 2009, 2011). Cultures were synchronized by overnight passage through L1 arrest, then grown for 57 h in liquid culture before using hypochlorite treatment to harvest young embryos (Baugh, 2009). For the fed time series, embryos were allowed to hatch in S-complete buffer so they enter L1 arrest, and 24 h after hypochlorite treatment they were fed with 25 mg/mL *Escherichia coli* HB101 in liquid culture. They were collected at the indicated time points thereafter and washed three times by centrifugation. For the starved time series, the same culture procedure was followed, except embryos were cultured in S-complete plus 25 mg/mL HB101 for 16 h, so they hatched and initiated L1 development, then the HB101 was washed away three times by centrifugation and they were cultured in S-complete and collected at the indicated timepoints thereafter. Each time series was collected in three biological replicates. TRIzol was used for RNA preparation (Invitrogen). Transcript counts were first normalized between samples by average spike-in positive control transcript counts, and 43 target gene transcript counts were further normalized by the sum of all 43 target gene transcript counts within each replicate. Two-way analysis of variance (ANOVA) between conditions (fed and starved) and time (0–12 h) were performed on normalized transcript counts with JMP 8. Genes with a $P_{\text{interaction}} > 0.0001$ or maximum transcript abundance below 2000 were excluded from clustering. Normalized transcript counts of the remaining genes were $\log_2$ transformed and mean centered over both time series, then hierarchically clustered based on single linkage in Cluster 3.0, and visualized in Java TreeView 1.1.6r3.

Destabilized YFP reporter gene analysis

Transcriptional reporters of insulin-like genes were constructed by fusing the promoter region, defined as the sequence upstream of the translational start site (5 kb maximum) of each gene (see Table S1), to YFP::PEST (Baugh et al., 2009). Plasmid pPDMM051 containing a wild-type *unc-119* gene was used as co-injection and selection marker. *unc-119(ed4)* worms were injected by standard microinjection protocol, and transgenic worms were screened for rescue of uncoordinated phenotype. Consistent expression patterns were confirmed among independent transgenic alleles, and one was chosen for further analysis for each construct. Identification of amphid neurons was aided by DiI (Invitrogen, D-282) or DiD (Invitrogen, D-307) staining (Fig. S1). YFP reporter strains were stained with 10 ng/μL DiI or DiD for 2–3 h at room temperature, and then paralyzed with sodium azide and examined on a fluorescent compound microscope on an agarose pad.

Quantitative imaging of YFP reporter genes

Larvae were cultured in S-complete with 25 mg/mL *E.coli* HB101 at 21 °C until gravid, embryos were collected by hypochlorite treatment, and they were resuspended at 5 eggs/μL at 21 °C in S-complete on a tissue culture roller drum. Embryos were cultured in S-complete without *E.coli* for 24 h and then 25 mg/mL *E.coli* HB101 was applied (feeding), or in S-complete with 25 mg/μL *E.coli* HB101 for 24 h and then *E.coli* was washed away three times by centrifugation in S-basal (starvation). Worms were scored at 0, 1.5, 3 and 6 h after adding or removing food. Worms were paralyzed with 10 mM sodium azide, mounted on agarose pads, and approximately 20 individuals were imaged at each time point on a compound fluorescence microscope with a 100× oil immersion objective. Pixel intensity of the intestinal cells or ASI was quantified from TIFF files in ImageJ. The whole procedure was repeated three times to produce three biological replicates.

Fig. 1. Comprehensive mRNA expression analysis of insulin-like genes during L1 arrest and recovery reveals nutrient-dependent regulatory dynamics. The NanoString nCounter platform was used to measure transcript abundance (*y*-axis, arbitrary units) over time (*x*-axis, hours) in fed (green) and starved (red) conditions. Error bars reflect the standard deviation of three biological replicates. *ins-13* is not included since the probe sequence used is not specific to that gene. The insulin-like receptor, *daf-2*, its effector, the FOXO transcription factor *daf-16*, and the DAF-16 target *sod-3* are also included for reference.

Phenotypic analysis of development

2000–5000 embryos were plated on each of two 10 cm NGM plates seeded with *E.coli* OP50 and cultured at 20 °C for 3–4 days (depending on the strain), and embryos were collected by hypochlorite treatment and resuspended at 1 egg/μL and cultured for 24 h in S-basal on a tissue culture roller drum. 1000 arrested L1s were put on 10 cm NGM plate seeded with *E.coli* OP50. After culturing for a defined period of time at a defined temperature, worms were washed off the plate and examined. *ayIs7*[*Phlh-8::GFP*] was used to score the number of M lineage cells (Harfe et al., 1998). Worms were paralyzed with 10 mM sodium azide, mounted and scored on an agarose pad. To measure body length, worms were instead put on an NGM plate without *E.coli*, and pictures were taken on a stereomicroscope and analyzed using WormSizer as previously described (Moore et al., 2013). All assays were repeated at least three times.

Starvation survival assay

5000 embryos were suspended in 5 mL virgin S-basal (not including ethanol or cholesterol) at 1 egg/μL in a 16 mm glass test tube on a tissue culture roller drum. Test tubes were rotated at a speed of 28 rpm at 21 °C. At each time point, 300 μL was removed and approximately 100 animals were examined on a slide on a dissecting microscope. Individuals that displayed spontaneous movement were considered alive. All assays were repeated at least three times. The median survival time for each trial was determined by fitting a curve with logistic regression, as previously described (Artyukhin et al., 2013), assuming a normal probability distribution for the time of death. An unpaired, two-tailed t-test was performed to compare median survival times between each mutant strain and *wild-type*. For display, replicates were averaged and a curve was fit with logistic regression.

Heat resistance assay

Embryos were collected by hypochlorite treatment and resuspended at 1 egg/μL in virgin S-basal (not including ethanol or cholesterol) in a 16 mm glass test tube and incubated on a tissue culture roller drum at 28 rpm and 21 °C for 24 h. Arrested L1 larvae were heated to 35 °C for 6 h while shaking at 180 rpm, then allowed to recover at 21 °C overnight. Animals capable of spontaneous movement were considered alive; approximately 100 larvae were scored per replicate.

Transgenic complementation and overexpression analysis

The transgenic rescue constructs include the 5′ intergenic region, the coding region and ~1 kb 3′ intergenic region for each gene (Table S2). Constructs were PCR amplified from N2 genomic DNA and purified using Qiagen columns. Individual rescue constructs were injected at a final concentration of 45 ng/μL, or a pool of 4 genes at ¼ dosage (11 ng/μL) each, or 45 ng/μL PvuII digested N2 genomic DNA (a negative control). Co-injection markers include 1 ng/μL pCFJ90 [*Pmyo-2::mCherry*], 45 ng/μL pBCN21-R4R3 [*Prpl-28::puroR::unc-54*_UTR] and additional 45 ng/μL PvuII digested N2 genomic DNA. Transgenic animals were generated by standard micro-injection protocol, and *ins-4, 5, 6(hpDf761); daf-28 (tm2308); ayIs7* [*Phlh-8*::*GFP*] worms were injected. Two independent transgenic alleles were selected for further analysis.

For the starvation survival assay, 5000 embryos were suspended in 5 mL virgin S-basal (not including ethanol or cholesterol) at 1 egg/μL in a 16 mm glass test tube. Test tubes were held on a tissue culture roller drum at 28 rpm and 21 °C. At each time point, worms were examined on a slide on a compound fluorescent microscope. Individuals that displayed spontaneous movement were considered alive. Bulk survival (live worms/total worms) over time is plotted in Fig. 7A. In addition to scoring live/dead, the frequency of mCherry-positive and -negative worms was scored among survivors. The relative frequency of

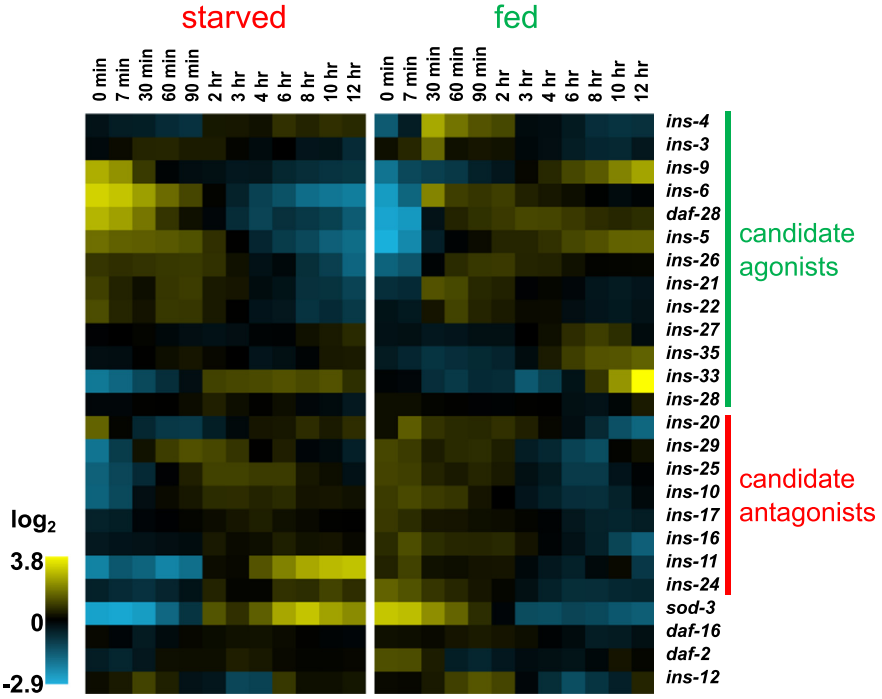

Fig. 2. Clustering insulin-like genes by mRNA expression dynamics reveals two major patterns of regulation. Genes that were reliably detected (max abundance greater than 2000) and displayed significantly different expression dynamics between fed and starved conditions (two-way ANOVA $P_{interaction} < 10^{-4}$, with no correction for multiple testing) were subjected to hierarchical clustering after $\log_2$ mean normalization. Yellow and blue reflect above and below average expression, respectively.

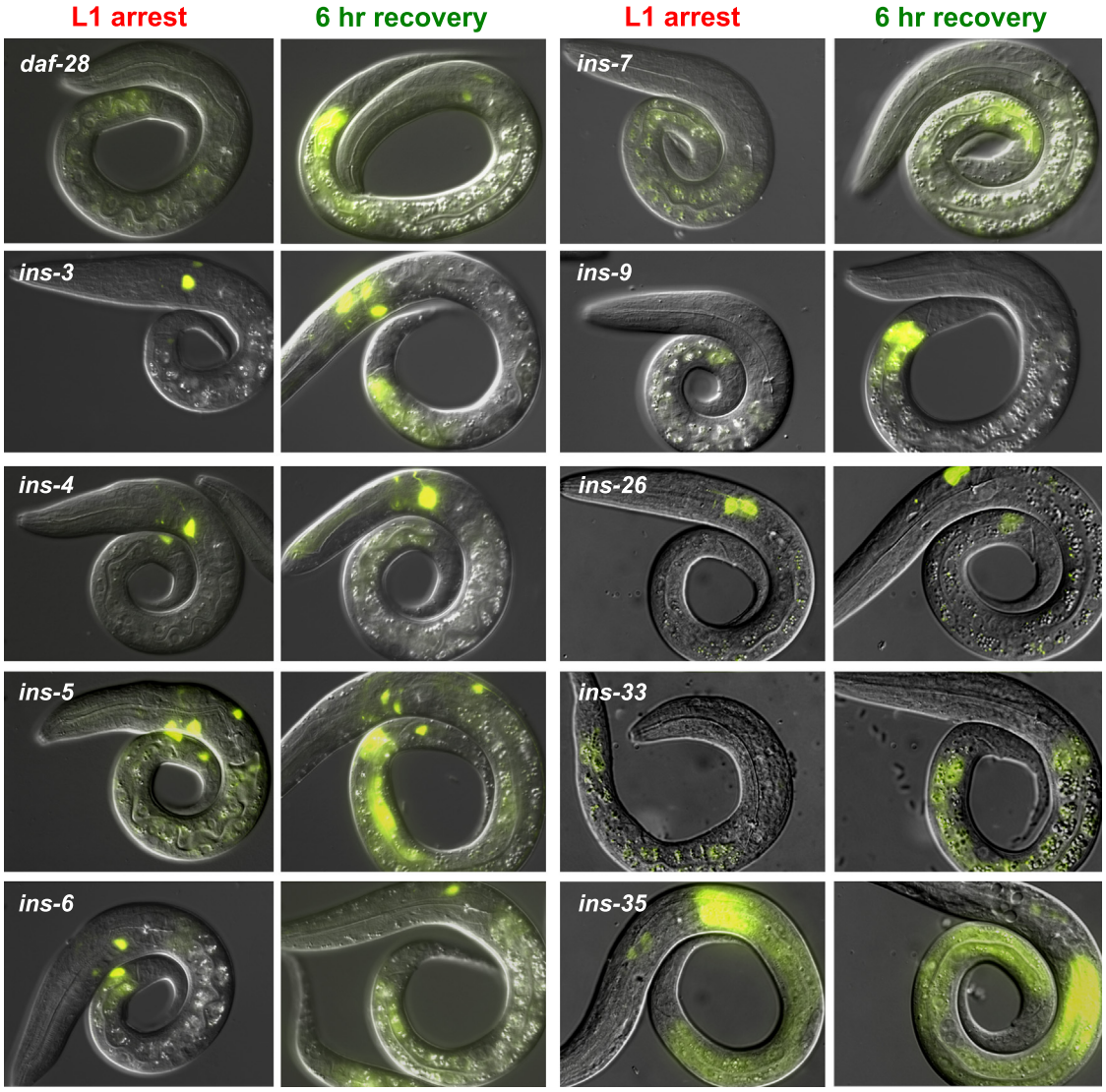

Fig. 3. Destabilized YFP reporter gene analysis reveals chemosensory neurons and intestine as primary sites of expression in L1 larvae. Representative images are shown for ten candidate agonists during L1 arrest and after 6 h recovery. Different exposure times were used for different reporter genes, and brightness of individual images was adjusted to obtain uniform background.

mCherry-positive worms among survivors was normalized within each strain to the frequency on day 1 of the experiment, and it is plotted in Fig. 7B. Approximately 100 total survivors were scored at each timepoint in each replicate.

For the M cell division assay during starvation, embryos were suspended in 3 mL S-basal (including 0.1% ethanol and 5 ng/μL cholesterol) at 1 egg/μL in a 16 mm glass test tube. Test tubes were placed on a tissue culture roller drum at 28 rpm and 21 °C. Worms were starved for 10 days before they were examined on a slide on a compound fluorescent microscope. Individuals that displayed spontaneous movement were considered alive, and whether or not the M cell had divided was scored in approximately 100 living mCherry-positive worms per replicate.

Results and discussion

mRNA expression analysis during entry into and recovery from L1 arrest

We used the nCounter platform to measure insulin-like mRNA expression over time during entry into and recovery from L1 arrest (Geiss et al., 2008). Twelve time points were collected over 12 h for each time series, with dense sampling early to capture rapid changes in expression. Total RNA prepared from whole worms was hybridized to a codeset containing probes for all 40 insulin-like genes as well as *daf-2*/InsR, *daf-16*/FOXO and the *daf-16* target *sod-3*, as previously described (Baugh et al., 2011). For L1 arrest recovery, larvae were arrested by hatching without food for approximately 12 h, and then synchronously recovered by feeding (recovery time zero). For entry into L1 arrest, larvae were hatched with food and allowed to develop for approximately 6 h, and then food was washed away (starvation time zero) to initiate starvation and developmental arrest. This approach is different from other studies of gene expression during L1 arrest, where larvae hatch without food (Baugh et al., 2009; Cui et al., 2013; Maxwell et al., 2012, 2014; Stadler and Fire, 2013), but it increases population synchrony during arrest entry, improving temporal resolution. The behavior of genes expected to be up-regulated during L1 arrest (e.g., *sod-3*) shows that this alternative approach produced comparable results to the traditional approach (Fig. 1). Furthermore, the correlation coefficient comparing the expression of all 43 genes between recovery time zero (~12 h L1 arrest by the traditional approach) and starvation time 12 h (12 h L1 arrest by

the alternative approach) is 0.92, indicating a strong correlation. Nonetheless, expression of genes up-regulated by initial feeding may be higher at starvation time zero than it would be in animals that hatched without food (e.g., *daf-28*), and such expression may persist for some genes in the starvation time series (e.g., *ins-33*).

Probes for *daf-2*/InsR, *daf-16*/FOXO and *sod-3* were included for reference in the nCounter codeset. We previously reported that several components of the insulin-like signaling pathway are up-regulated during L1 arrest, but microarray signal for *daf-2* was too low for assessment (Baugh et al., 2009). The nCounter results show

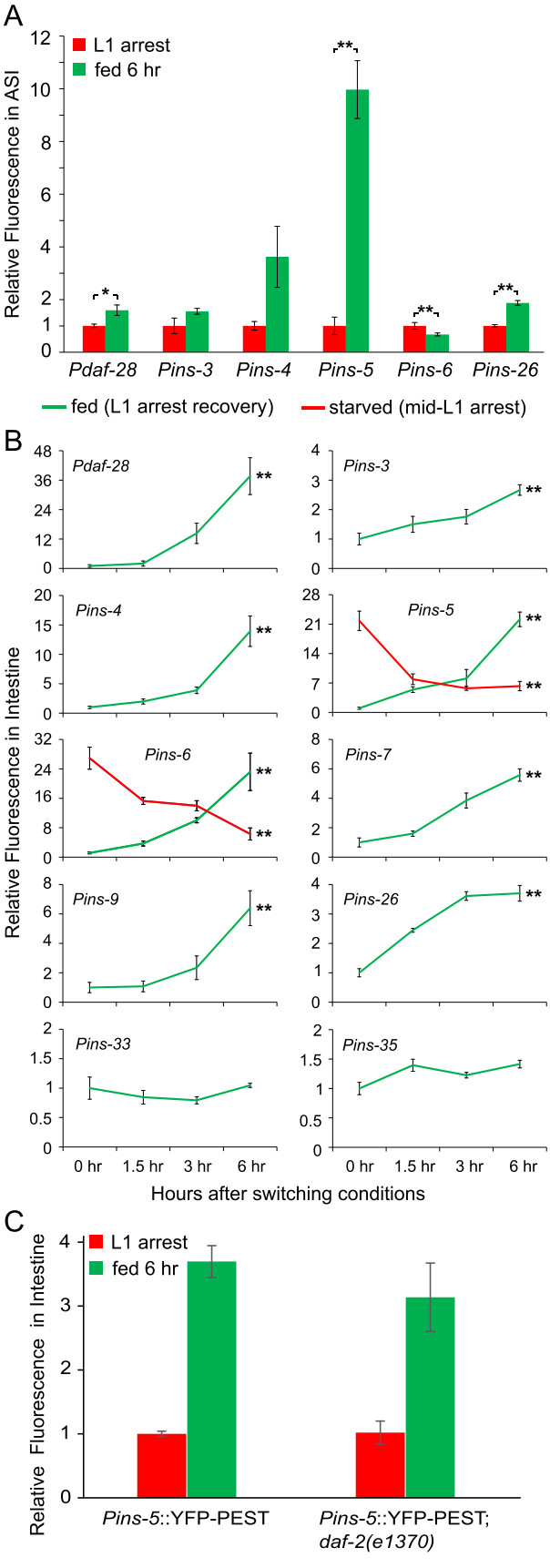

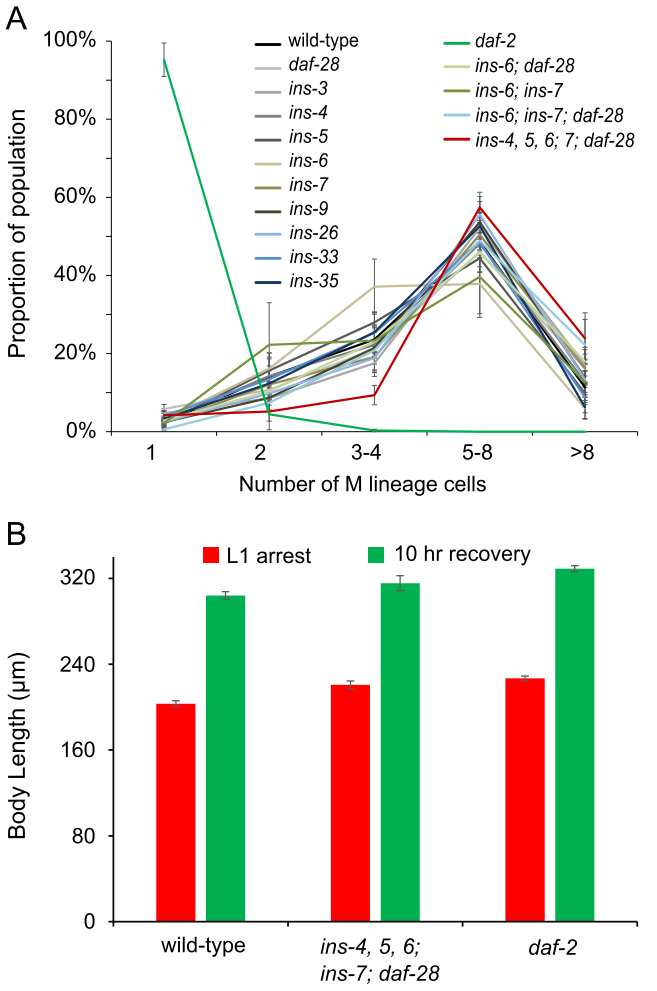

Fig. 5. Disruption of candidate agonists does not have detectable effects on cell division or growth rate in L1 larvae. (A) The proportion of larvae with 1, 2, 3–4, 5–8 and >8 M lineage cells after 10 h recovery from L1 arrest at 25 °C is plotted for a variety of single and compound deletion mutants. Approximately 200 larvae were scored per replicate. (B) Body length is plotted for wild-type, *daf-2(e1370)* and a strain with 5 candidate agonists deleted during L1 arrest and after 10 h recovery at 25 °C. 50–100 larvae were imaged per replicate per timepoint. (A and B) All strains have *ayIs7* [*Phlh-8*::GFP] in the background. Average and standard error of the mean are plotted for at least three biological replicates.

Fig. 4. Quantitative reporter gene analysis demonstrates nutritional control of transcription and reveals the intestine as a major site of transcriptional regulation. (A) Relative YFP fluorescence intensity in ASI chemosensory neurons is plotted for six candidate agonists expressed in ASI during L1 arrest and after 6 h recovery. Two-tailed, unpaired t-tests were used to assess statistical significance ($^{*}P<0.05$; $^{**}P<0.01$; no correction for multiple testing). (B) Relative YFP fluorescence intensity in the intestine is plotted for ten candidate agonists during L1 arrest and over time during recovery (green). *ins-5* and *ins-6* reporters were also subjected to starvation during the mid-L1 stage (red). One-way ANOVA was used to assess statistical significance ($^{**}P<0.01$; no correction for multiple testing). (C) Relative fluorescence in the intestine of an integrated *ins-5* reporter gene is plotted for L1 arrest and 6 h recovery in a wild-type and *daf-2(e1370)* background. The *daf-2* mutant did not have a significant effect on reporter expression. (A–C) Intensity was normalized to L1 arrest values for each reporter. The average and standard error of the mean are plotted for three biological replicates; approximately 20 animals were analyzed per replicate per time point.

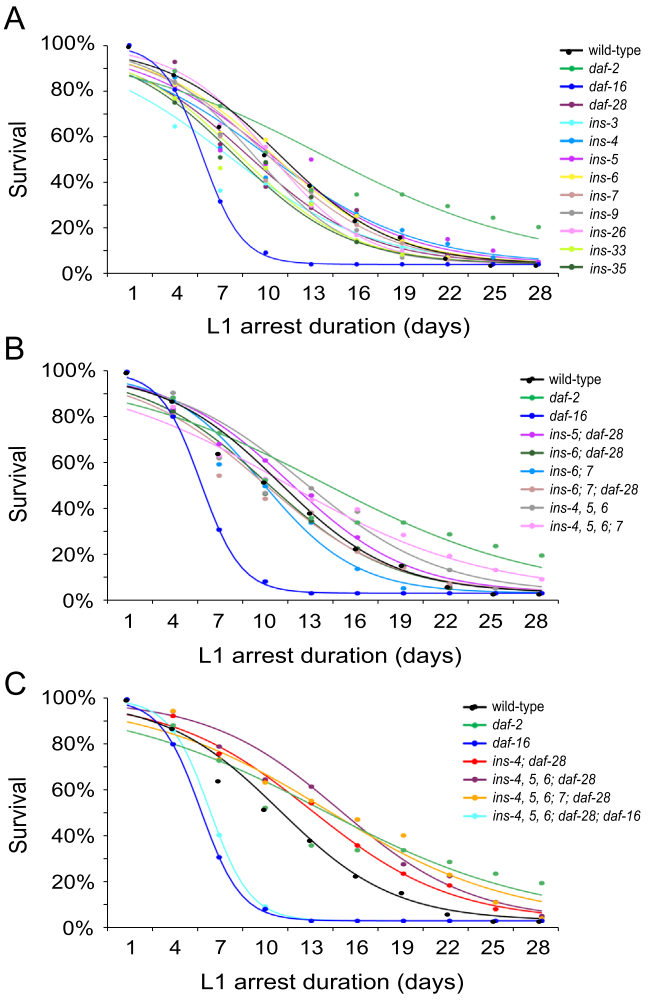

Fig. 6. Simultaneous disruption of *ins-4* and *daf-28* increases survival of L1 arrest. (A) L1 arrest survival is plotted over time (days) for deletions affecting each of ten candidate agonists as well as wild-type, *daf-2(e1370)* and *daf-16(mgDf50)*. (B and C) L1 arrest survival is plotted over time for various compound deletion mutants as well as the same controls from A. (A–C) All strains have *ayIs7* [*Phlh-8*::GFP] in the background. Survival was assessed in 5 mL virgin S-basal (no cholesterol or ethanol) at a density of 1 worm/μL at 21 °C in a 16 mm glass test tube maintained on a tissue culture roller drum. Approximately 100 larvae were scored per replicate per time point; animals capable of spontaneous movement were considered alive. A logistic regression of mean survival from at least three biological replicates is plotted.

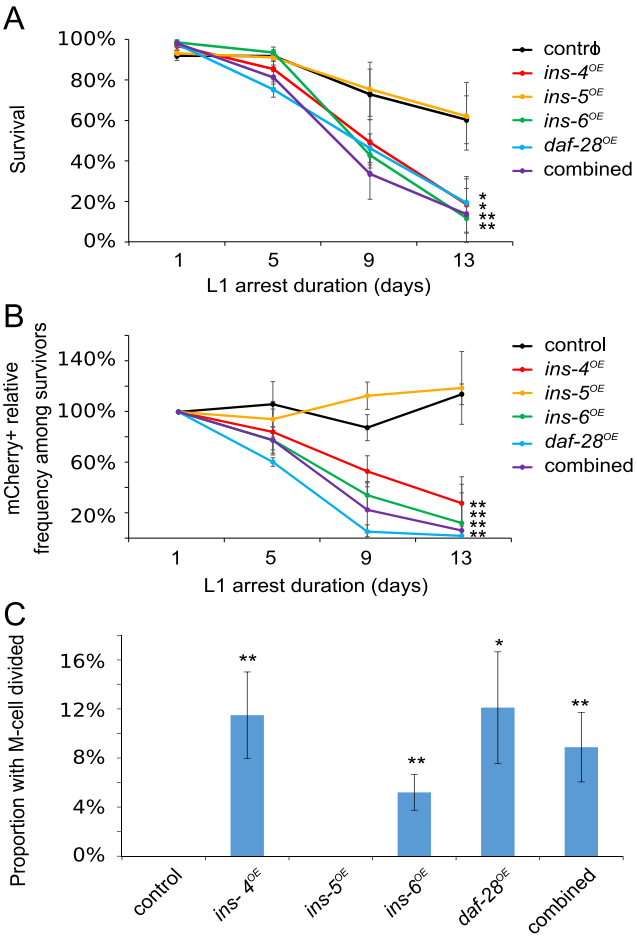

Fig. 7. Over-expression of *ins-4*, *ins-6* or *daf-28* causes an L1 arrest-defective phenotype, affecting starvation survival and M cell division. (A) Population-wide survival during L1 arrest is plotted over time (days) for *ins-4, ins-5, ins-6(hpDf61); daf-28(tm2308)* worms over-expressing (OE) *ins-4*, *ins-5*, *ins-6*, *daf-28* or a combination of all four genes from an extrachromosomal array. Statistical significance was assessed by two-way ANOVA comparing each over-expression genotype to the control with time and genotype as factors ($^{*}P_{\text{interaction}} < 0.05$, $^{**}P_{\text{interaction}} < 0.01$). (B) The relative frequency of transgenic (mCherry^{+}) worms among survivors is plotted over time during starvation for the same strains as in A. For each strain and each replicate, the frequency on day 1 of the experiment was used for normalization. A one-way ANOVA with time as the factor was used to assess statistical significance ($^{**}P_{\text{time}} < 0.01$). (C) Over-expression of *ins-4*, *ins-6* or *daf-28* causes the M cell to divide during L1 starvation. The proportion of surviving mCherry^{+} individuals with at least one M cell division after ten days of L1 starvation in S-basal is plotted for the same strains as in A and B. An unpaired, two-tailed t-test comparing each genotype to the control was used to assess statistical significance ($^{**}P < 0.01$, $^{*}P = 0.06$). (A–C) Approximately 100 individuals were scored at each time point in each replicate. Average and standard error of the mean are plotted from two biological replicates including two independent transgenic alleles for each genotype (four replicates total). All strains have *ayIs7*[*Phlh-8::GFP*] in the background. The control carries only transformation markers in the extrachromosomal array in the same *ins-4, ins-5, ins-6(hpDf61); ayIs7; daf-28*(*tm2308*) background as the other strains.

clear, significant up-regulation of *daf-2* in starved L1 larvae (Fig. 1; Table 1). The insulin receptor is also up-regulated during starvation in *Drosophila* and mammals, suggesting that feedback regulation via FOXO elevates sensitivity to signaling (Puig and Tjian, 2005). Consistent with this model, we also see mild but significant up-regulation of *daf-16* during L1 arrest (Fig. 1; Table 1). The superoxide-dismutase *sod-3* is a direct target of *daf-16* (Oh et al., 2006), and, as expected, it is clearly up-regulated in starved larvae and down-regulated in fed larvae (Fig. 1).

The majority of insulin-like genes show dynamic, nutrient-dependent expression. We used two-way analysis of variance (ANOVA) to assess statistical significance of the effects of nutrition and time as well an interaction between the two (Table 1). Unfortunately, signal for eleven genes was deemed too low for reliable assessment. In addition, the 3′ untranslated region of *acdh-2* overlaps with *ins-13*, and we found that the abundant expression of *acdh-2* dominates the *ins-13* probe (data not shown), so these 12 genes were not subjected to ANOVA. Of the 28 insulin-like genes we were able to obtain reliable data for, 23 (82%) were significantly affected by nutrition ($P_{\text{nutrition}} < 10^{-4}$ with no correction for multiple testing). This result reveals a pervasive effect of nutrient availability on insulin-like gene expression. Furthermore, 21 (75%) insulin-like genes were significantly affected by time ($P_{\text{time}} < 10^{-4}$ with no correction for multiple testing), reflecting the temporal resolution of our data and the dynamic nature of insulin-like signaling. The effects of nutrition and time are interdependent, and 22 (79%) insulin-like genes showed a significant interaction between the two factors ($P_{\text{interaction}} < 10^{-4}$ with no correction for multiple testing), indicating that the dynamics of their response to one condition differs from the other.

Table 1
Two-way ANOVA for mRNA expression dynamics in fed and starved conditions based on nCounter analysis. *P*-values for each factor (nutrient availability, time and their interaction) are reported. P-values considered significant (less than 0.0001 with no correction for multiple testing) are in bold. Genes with maximum transcript abundance less than 2000 and *ins-13* were excluded.

Gene	Two-way ANOVA			Prior characterization
	$P_{nutrition}$	P_{time}	$P_{interaction}$	
daf-2	**2.3E-18**	**8.1E-05**	**5.3E-22**	
daf-16	**1.7E-06**	**8.4E-08**	**2.0E-07**	
sod-3	**8.5E-06**	**7.3E-07**	**2.6E-21**	
daf-28	**5.8E-28**	4.4E-03	**6.5E-25**	agonist: dauer[a,b,c,i,j], reproductive span[j]
ins-1	1.1E-02	**1.4E-09**	5.1E-01	antagonist: dauer[b,d,i,j]; agonist: thermotolerance[j]
ins-2	**5.0E-19**	6.6E-04	1.3E-03	
ins-3	**1.2E-07**	**1.5E-12**	**9.2E-06**	agonist: germline proliferation[e], dauer [i]; antagonist: dauer[j]
ins-4	9.3E-02	**1.9E-15**	**1.3E-22**	agonist: dauer[c,i,j]
ins-5	**6.5E-09**	1.5E-01	**1.1E-19**	agonist: dauer[j]
ins-6	**1.4E-09**	**3.3E-15**	**6.8E-18**	agonist: dauer[b,c,i,j], lifespan[j], reproductive span[j]
ins-9	**8.4E-22**	**1.1E-16**	**1.1E-23**	
ins-10	**5.2E-12**	**8.6E-07**	**4.4E-25**	agonist: dauer[j]
ins-11	**6.8E-25**	**1.0E-21**	**3.6E-23**	antagonist: aging[f]; agonist: dauer[j]
ins-12	3.3E-03	**1.2E-05**	**1.5E-06**	antagonist: dauer entry[j]; agonist: dauer exit[j]
ins-14	**3.5E-11**	**3.4E-11**	6.9E-02	agonist: dauer[j]
ins-16	**7.7E-25**	**1.2E-10**	**3.1E-14**	
ins-17	**1.6E-28**	**2.8E-06**	**2.2E-18**	antagonist: dauer[g]
ins-18	**2.4E-13**	**1.0E-04**	1.6E-01	antagonist: dauer[d,h,i,j]
ins-20	**3.0E-20**	**8.5E-08**	**5.4E-12**	antagonist: pathogen resistance[j]
ins-21	**4.6E-12**	**2.1E-11**	**2.7E-07**	agonist: dauer[j]
ins-22	**1.8E-15**	**9.4E-12**	**1.9E-05**	agonist: dauer[j]
ins-24	**1.3E-15**	**2.5E-05**	**4.3E-12**	
ins-25	**4.9E-10**	2.8E-03	**3.1E-12**	
ins-26	1.2E-01	**1.3E-11**	**9.5E-12**	agonist: dauer[j]
ins-27	**2.2E-08**	**6.4E-12**	**3.0E-08**	agonist: thermotolerance, pathogen resistance[i]
ins-28	**8.7E-11**	4.7E-03	**4.3E-08**	
ins-29	6.5E-01	**1.8E-08**	**1.1E-10**	
ins-30	**1.3E-34**	2.2E-01	5.7E-03	
ins-33	**6.7E-17**	**1.2E-17**	**7.5E-15**	agonist: germline proliferation[e], dauer[j]
ins-34	**1.3E-14**	4.8E-02	6.3E-02	
ins-35	**1.5E-15**	**7.2E-25**	**2.7E-23**	agonist: dauer[j]

[a] Patel et al. (2008).
[b] Cornils et al. (2011).
[c] Li et al. (2003).
[d] Pierce et al. (2001).
[e] Michaelson et al. (2010).
[f] Kawano et al. (2006).
[g] Matsunaga et al. (2012a).
[h] Matsunaga et al. (2012b)
[i] Hung et al. (2014).
[j] Fernandes de Abreu et al. (2014).

Insulin-like gene expression patterns are complex, varying over time and between conditions. Consistent with functioning as an agonist to promote dauer bypass (Li et al., 2003), *daf-28* is clearly up-regulated by feeding and down-regulated by starvation (Fig. 1). Several other genes are also up-regulated by feeding. However, whereas *daf-28* up-regulation is early and persistent, others are early and transient (e.g., *ins-4*), gradual (e.g., *ins-5* and *ins-9*) or late (e.g., *ins-33*). Consistent with functioning as an antagonist to promote dauer formation (Matsunaga et al., 2012b), *ins-17* is up-regulated by starvation and down-regulated by feeding (Fig. 1). Another antagonist (Matsunaga et al., 2012a), *ins-18*, is also up-regulated by starvation, but it is early and transient. In contrast, *ins-11* is up-regulated gradually during starvation. Despite variation in dynamics, these results reveal a correlation between nutrient-dependent expression and gross function (agonist vs. antagonist), suggesting we can use the results of our expression analysis for functional predictions.

We used the results of two-way ANOVA together with cluster analysis to classify insulin-like genes as candidate agonists or antagonists. Our rationale is that agonists and antagonists are likely to be up-regulated in response to feeding and starvation, respectively. We only clustered genes with a P-value for the nutrition-by-time interaction below 10^{-4}. This requires a distinct temporal response to each condition (fed and starved). Two major patterns are evident after clustering: (1) genes up-regulated by feeding and down-regulated by starvation, including the prototypical agonist *daf-28*, and (2) genes down-regulated by feeding and up-regulated by starvation, including the prototypical antagonist *ins-17* (Fig. 2). We classified genes in each of these clusters as agonists or antagonists, respectively, resulting in thirteen candidate agonists and eight candidate antagonists. Visual inspection of the expression of each gene confirms its classification (Fig. 1). *ins-12* has a complex expression pattern, and it did not cluster with either group, so we did not classify it despite a significant nutrition-by-time interaction.

Our classification of candidate agonists and antagonists correctly assigned most genes of known function. Genes reported to function as agonists or antagonists in different contexts are not considered here (of which we classified *ins-3* and *ins-11* as agonist and antagonist, respectively) (Fernandes de Abreu et al., 2014). Out of ten genes reported to function as agonists in any publication that we also classified, we classified all ten as agonists based on expression in L1 larvae (Fig. 2; Table 1). Moreover, there appears to be a correlation between late or sustained expression in fed L1

larvae and promoting dauer bypass (e.g., *daf-28*, *ins-33* and *ins-35* with *ins-9* as an exception) (Fernandes de Abreu et al., 2014). *ins-7* is known to function as an agonist to promote aging (Murphy et al., 2003), but the previous expression analysis suggests it is specific to L4 larvae and adults (Baugh et al., 2011). Consistent with this interpretation, expression in L1 larvae is too low for differential expression to be reliably assessed so it was not classified. Out of three genes reported to function as antagonists in any publication that we also classified, we classified all three as antagonists based on expression in L1 larvae (Fig. 2; Table 1). *ins-18* is known to function as an antagonist in dauer entry (Fernandes de Abreu et al., 2014; Matsunaga et al., 2012a), and we previously found that it is up-regulated in L1 arrest and dauer formation (Baugh et al., 2011). It is more highly expressed in L1 arrest than recovery here, but it did not show a significant nutrition-by-time interaction in ANOVA, so it was not clustered or classified as an antagonist. Alternatively, we could have clustered all genes found to be significant by two-way ANOVA (as opposed to only those with a significant nutrition-by-time interaction). That would have classified *ins-18* as an antagonist, but it would have also classified other insulin-like genes with less confidence. For example, *ins-2* and *ins-34* both decrease over time during recovery (Fig. 1), but this appears to be due to embryonic expression rather than up-regulation during starvation (Baugh et al., 2011), and there is no evidence that either functions as an antagonist (Fernandes de Abreu et al., 2014). In conclusion, meta-analysis of the literature suggests that our functional predictions suffer a very low false-positive rate, though not every insulin-like gene of known function can be classified based on expression in L1 larvae.

Destabilized reporter gene analysis during L1 arrest and recovery

We constructed destabilized YFP transcriptional reporter genes to complement temporal analysis of mRNA expression for ten candidate agonists. In addition to nine of the candidate agonists identified, we also included a reporter for *ins-7* since it is known to function as an agonist in a different context (Murphy et al., 2003). We fused non-coding sequence upstream of each insulin-like gene to YFP carrying the PEST sequence from mouse ornithine decarboxylase on its C-terminus for destabilization. We previously characterized this reporter protein in L1 arrest, confirming that it is uniformly destabilized throughout the animal and has a greatly reduced half-life compared to ordinary GFP-based reporters (Baugh et al., 2009).

Reporter expression is consistent with neuroendocrine control of L1 arrest and recovery. In particular, six of ten reporters were expressed in the chemosensory neuron ASI, three of those were also expressed in chemosensory neuron ASJ and another in chemosensory neuron ASK (Table 2 and Fig. 3). In addition, reporters for *ins-26* and *ins-35* were expressed in chemosensory neurons ASE and AWC. Chemosensory neuron function is known to affect L1 arrest survival and constitutive arrest of *daf-2*/InsR mutants (Lee and Ashrafi, 2008; Vowels and Thomas, 1992). Furthermore, *daf-28* is known to be expressed in ASI and ASJ (Li et al., 2003), though not this early, and these neurons are also known to regulate dauer formation (Bargmann and Horvitz, 1991). Our expression analysis during L1 arrest and recovery further suggests that chemosensory neurons, ASI and ASJ in particular, contribute to regulation of L1 arrest. In addition, each of the six reporters expressed in ASI was also expressed in the tail interneuron PVT (Table 2). This striking correlation suggests that PVT may provide neuroendocrine control of development like ASI, though it is not known to be sensory and such endocrine function has not been described.

Reporter expression also suggests that the intestine provides systemic control of L1 arrest and recovery. All ten reporter genes analyzed were expressed in the intestine (Fig. 3; Table 2). Intestinal expression was generally weak and often only visible in the posterior during L1 arrest, but it appeared brighter during recovery and expanded to anterior intestinal cells. Like the nervous system, the intestine is known to be an important site of action for the insulin-like signaling pathway during aging and L1 arrest survival (Baugh, 2013). However, the expression, secretion and function of insulin-like peptides has generally focused on neuronal cells (Cornils et al., 2011; Kao et al., 2007; Lee and Ashrafi, 2008; Li et al., 2003; Matsunaga et al., 2012a). These results suggest that the intestine also provides endocrine control of L1 arrest and

Table 2
Expression patterns of 10 candidate agonists in arrested and fed L1 worms based on destabilized YFP transcriptional reporter gene analysis. DiI or DiD staining was used to help identify amphid chemosensory neurons (Fig. S1).

	Head Neurons	Tail Neurons	Intestine	Other
L1 arrest				
daf-28	ASI, ASJ	PVT	posterior (weak)	head neurons
ins-3	ASI, ASJ (major), URX	PVT	posterior (weak)	
ins-4	ASI (major), ASJ, URX	PVT	posterior (weak)	tail cells
ins-5	ASK (major), ASI, RID	PVT	whole, stronger in posterior	tail cells; tail neurons
ins-6	ASI	PVT	posterior (weak)	head muscles; coelomocytes; head neurons; tail cells
ins-7	RID		posterior (weak)	head neurons
ins-9			posterior (weak)	head neurons
ins-26	ASI, ASE, AWC	PVT	posterior	tail cells
ins-33			posterior and anterior	head muscles; head neurons; tail cells
ins-35	ASE, AWC		whole, stronger in anterior	head neurons
Fed 6 h				
daf-28	ASI, ASJ	PVT	whole, stronger in posterior	head neurons
ins-3	ASI, ASJ (major), URX	PVT	whole, stronger in posterior	
ins-4	ASI (major), ASJ, URX	PVT	posterior	tail cells; hypodermis (rare)
ins-5	ASK, ASI (major), RID	PVT	whole, stronger in posterior	tail cells; tail neurons
ins-6	ASI	PVT	posterior	head muscles; ceolomocytes; head neurons; tail cells
ins-7	RID		posterior and anterior	head neurons; tail cells
ins-9			posterior	head neurons; tail cells
ins-26	ASI, ASE, AWC	PVT	posterior	tail cells
ins-33			whole, stronger in posterior and anterior	head muscles; head neurons; tail cells
ins-35	ASE, AWC		whole, stronger in anterior	head neurons

recovery, which would be analogous to mammals in that the pancreas is endodermal and the intestine is the sole endodermal organ in *C. elegans*. Our results are generally consistent with a previous comprehensive study, in which head neurons and intestine are found to be sites where most insulin-like genes are expressed in L1 stage larvae (Ritter et al., 2013).

Reporter gene analysis reveals nutritional control of transcription. By measuring mRNA steady-state levels, nCounter analysis cannot distinguish between regulation of transcription and transcript stability. Because we used promoter fusions, changes in reporter gene expression imply transcriptional regulation. Despite being candidate agonists, all ten reporters were expressed during L1 arrest (Fig. 3; Table 2). All ten were also expressed during recovery, and the patterns of expression generally did not change within 6 h – the exception being expansion within the intestine during recovery. We used image analysis to quantify reporter gene expression. Of the six reporter genes expressed in ASI, three were significantly up-regulated after 6 h recovery (Fig. 4A). In contrast, eight out of ten reporters were significantly up-regulated in the intestine, largely confirming the nCounter results (Fig. 4B). *ins-33* is expressed relatively late during recovery (Fig. 1), consistent with promoting germline proliferation (Michaelson et al., 2010), presumably accounting for the lack of reporter up-regulation observed within 6 h. However, it is unclear why the *ins-35* reporter was not up-regulated, but it could be that the appropriate regulatory elements were not included in the construct. Lack of intestinal up-regulation of *ins-33*, *ins-35* and other reporters not described here provide evidence that intestinal expression is a gene and condition-specific effect, as opposed to a property of the reporter construct used. We also examined reporter expression for *ins-5* and *ins-6* during entry into starvation (Fig. 4B). Both reporters were significantly down-regulated in the intestine, confirming that the reporter protein is destabilized and showing both positive and negative transcriptional control in the intestine.

The intestine appears to be the major site of transcriptional regulation of insulin-like gene expression in response to nutrient availability. Even in the limited cases where up-regulation was evident in ASI, intestinal up-regulation was substantially greater (Fig. 4). Multiple lines of evidence suggest that chemosensory neurons, ASI and ASJ in particular, regulate L1 arrest, presumably in response to environmental conditions (Baugh, 2013). However, such regulation could occur at the level of insulin-like peptide translation, maturation or secretion. Indeed, transcriptional reporters for seven of ten candidate agonists were expressed in chemosensory neurons during L1 arrest, suggesting a pool of mRNA and possibly protein is available for direct regulation.

Regulation of insulin-like gene expression

The insulin-like signaling pathway regulates transcription of individual insulin-like genes, creating feedback and causing the state of the pathway to spread between tissues (FOXO-to-FOXO signaling) (Matsunaga et al., 2012a; Murphy et al., 2003, 2007; Oliveira et al., 2009). It is therefore possible that up-regulation of insulin-like gene expression in the intestine could result from increased peptide secretion from chemosensory or other neurons. To test this hypothesis, we examined intestinal *ins-5* reporter expression during recovery in a *daf-2* mutant, but the mutation did not affect induction (Fig. 4C). This result suggests that intestinal up-regulation of *ins-5* does not depend on upstream insulin-like signaling, consistent with an autonomous response of the intestine to feeding.

We tried to identify *cis*-regulatory motifs associated with insulin-like genes classified as candidate agonists or antagonists. We used the software MEME to search for motifs enriched within each gene set, including 700 bp upstream of the translation start site for each gene (Bailey et al., 2009). Unfortunately we did not identify significantly enriched motifs in this unbiased analysis, possibly due to the fact that these gene sets are relatively small. We also scanned for the known consensus binding sites of transcription factors associated with insulin-like signaling and/or energy homeostasis (DAF-16/FOXO, SKN-1/NrF, PQM-1 and PHA-4/FOXA) using the software FIMO from the MEME suite (Tepper et al., 2013; Tullet et al., 2008; Zhong et al., 2010). Putative binding sites were identified, but there is no significant enrichment or depletion of these sites in candidate agonists, antagonists or insulin-like genes in general compared to the rest of the genome. In addition, we examined the modENCODE ChIP-seq data for DAF-16 (fed L4/young adult), SKN-1 (fed L1), PHA-4 (fed L1) and PQM-1 (fed L4/young adult) for peaks within 1 kb upstream of each insulin-like gene or the entire intergenic region (Niu et al., 2011). Again, there were no significant associations between putative binding and classification as either agonist or antagonist. Future work taking advantage of additional motifs and transcription factor binding data should be more informative.

Phenotypic analysis of deletion mutants during development

We sought to identify insulin-like genes that promote L1 development in response to feeding. We reasoned that insulin-like genes up-regulated in response to feeding were likely to have this function and phenocopy, though to a lesser extent, *daf-2*/InsR mutants. To test this hypothesis, we performed phenotypic analysis of deletion mutants, disrupting function of each of the ten candidate agonists for which we also performed reporter gene analysis. *ins-4*, *ins-5* and *ins-6* are within 6 kb of each other in a chromosomal cluster, and we also analyzed a deletion mutant (*hpDf761*) (Hung et al., 2014) that lacks all three genes, as well as a variety of mutant combinations.

We analyzed the developmental progression of a variety of single and compound deletion mutants. The proportion of animals in each developmental stage was scored at a time and temperature when nearly all wild-type animals have become adults and nearly all *daf-2(e1370)* mutants have arrested as dauer larvae (Fig. S2). With the exception of the *daf-28* mutant, none of the single mutants analyzed had a significant effect on developmental progression. *daf-28(tm2308)* is known to cause dauer formation (Patel et al., 2008), as observed, and we also observed enhancement of this phenotype by *ins-6(tm2416)*, as reported (Cornils et al., 2011). Unlike *daf-2* mutants, the dauer phenotype of *ins-6*; *daf-28* compound mutants is not temperature-sensitive, and it is transient (data not shown), as reported elsewhere (Hung et al., 2014). These results confirm published findings with respect to dauer formation, but they fail to uncover additional gross effects on larval development.

We analyzed developmental progression through the L1 larval stage during recovery from L1 arrest using a quantitative assay that is sensitive to subtle effects on cell division rate. There is a single M cell in early L1 larvae and during L1 arrest, and the M cell and its descendants go through a series of cell divisions during the latter half of the L1 stage (Sulston and Horvitz, 1977). The number of M cells per animal thus provides a relatively precise means of monitoring L1 development. *daf-2*/InsR mutants develop slower than wild-type in the L2 larval stage (Ruaud et al., 2011), and we found a significant delay in the rate of M cell lineage divisions in *daf-2(e1370)* during the L1 stage (Fig. 5A). However, none of the insulin-like gene mutants analyzed displayed a delayed M lineage division phenotype, including simultaneous disruption of *ins-4*, *ins-5*, *ins-6*, *ins-7* and *daf-28*, suggesting extensive functional overlap.

To complement analysis of cell division rate, we used quantitative imaging to analyze length during L1 arrest and after 10 h recovery (Moore et al., 2013). None of the single mutants analyzed

Table 3
Summary of L1 arrest survival results. Median survival was calculated using a logistic regression fit to each survival curve, and the average and standard deviation (S.D.) across biological replicates are reported for each genotype. The number of biological replicates is also indicated (n). A two-tailed, unpaired *t*-test was used to compute *P*-values for each strain compared to wild-type, except for those *P*-values labeled with * or #. *P*-values below 0.002 were considered significant, which corresponds to a 0.05 experiment-wide false discovery rate. A single deletion allele (*hpDf761*) was used for deletion of *ins-4*, *ins-5* and *ins-6*.

Genotype	Median survival	S.D.	*n*	*P*-value	
wild-type	10.3	1.2	16	N/A	
daf-2	13.1	1.2	4	<0.002	
daf-16	5.9	0.3	4	<0.0001	
daf-28	9.5	0.8	3	N.S.	
ins-3	7.4	2.4	3	N.S.	
ins-4	9.7	1.0	3	N.S.	
ins-5	10.6	2.3	3	N.S.	
ins-6	10.5	1.1	3	N.S.	
ins-7	9.8	0.9	3	N.S.	
ins-9	9.0	1.0	3	N.S.	
ins-26	10.2	1.8	3	N.S.	
ins-33	7.6	0.7	3	N.S.	
ins-35	7.9	0.6	3	N.S.	
ins-4; daf-28	13.6	1.7	6	<0.001	
ins-5; daf-28	11.7	0.5	3	N.S.	
ins-6; daf-28	9.6	0.9	5	N.S.	
ins-6; ins-7	9.8	0.8	3	N.S.	
ins-6; ins-7; daf-28	9.7	0.5	3	N.S.	
ins-4, 5, 6	12.4	0.5	3	N.S.	
ins-4, 5, 6; ins-7	12.4	1.3	3	N.S.	
ins-4, 5, 6; daf-28	14.7	2.1	6	<0.0001	1;*N.S.
ins-4, 5, 6; ins-7; daf-28	14.0	1.7	5	<0.0001	1;*N.S.
ins-4, 5, 6; daf-28; daf-16	6.4	0.3	3	<0.0001	2;#N.S.

N/A: not applicable; N.S.: not significant.
* compared to ins-4; daf-28.
# compared to *daf-16.*

displayed reduced growth during recovery from L1 arrest (Fig. S3). Furthermore, simultaneous disruption of *ins-4*, *ins-5*, *ins-6*, *ins-7* and *daf-28* also did not affect L1 growth rate (Fig. 5B). However, *daf-2(e1370)* also did not display reduced growth rate (Figs. 5B, S3), though *sma-9(wk55)* did (Fig. S3), as expected based on previous results (Moore et al., 2013). The fact that mutation of *daf-2*/InsR delayed M cell lineage division without affecting growth rate suggests that regulation of cell division and growth can be uncoupled in the L1 larval stage, as if insulin-like signaling regulates developmental events such as cell division independent of growth.

Phenotypic analysis of deletion mutants during L1 arrest

In addition to affecting the rate of development, reduction of *daf-2*/InsR function or insulin-like peptide secretion increases survival during L1 arrest (Baugh and Sternberg, 2006; Lee and Ashrafi, 2008). These results suggest basal agonistic signaling activity during L1 arrest, as if disruption of specific agonists could also increase starvation survival. We found, as expected, that *daf-2 (e1370)* and *daf-16(mgDf50)* mutants are starvation resistant and sensitive, respectively (Fig. 6A, Table 3). However, deletion of each of the ten candidate agonists investigated had no significant effect on L1 arrest survival. Furthermore, a variety of double and triple mutant combinations also did not have a significant effect (Fig. 6B; Table 3).

In contrast, simultaneous disruption of *ins-4* and *daf-28* significantly increased starvation survival (Fig. 6C, Table 3), consistent with these insulin-like peptides functioning as *daf-2*/InsR agonists. Epistasis analysis with *daf-16*/FOXO confirms that increased starvation survival depends on *daf-16*, as expected for *daf-2*/InsR agonists (Fig. 6C). Disruption of *ins-5*, *ins-6* and *ins-7* in addition to *ins-4* and *daf-28* did not have an additional, significant effect on survival (Table 3). Together with the lack of single mutant effects for the other genes, this result suggests that *ins-4* and *daf-28* function relatively specifically to influence survival during L1 arrest.

We wondered if loss of *ins-4* and *daf-28* function affects stress resistance beyond starvation survival. We confirmed that *daf-2 (e1370)* is heat resistant during L1 arrest (Munoz and Riddle, 2003), but loss of *ins-4* and *daf-28* did not have a significant effect on resistance (Fig. S4), suggesting that *ins-4*; *daf-28* mutants are not generally stress resistant. Our results are consistent with thermotolerance being affected by a distinct set of insulin-like genes (Fernandes de Abreu et al., 2014), though it is unclear how such specificity occurs.

Transgenic complementation and phenotypic analysis of over-expression

Transgenic complementation confirms that mutations in *ins-4* and *daf-28* affect survival of L1 arrest. We injected wild-type copies of *ins-4*, *ins-5*, *ins-6* and *daf-28* alone and in combination into an *ins-4, ins-5, ins-6*; *daf-28* mutant and scored starvation survival. Scoring survival population-wide (independent of whether each individual carried the extrachromosomal array) revealed that *ins-4*, *daf-28* or *ins-6* alone rescues the mutant phenotype (Fig. 7A). In fact, over-expression of these transgenes appears to reduce survival below wild-type, consistent with the *daf-16* loss-of-function starvation-sensitive phenotype (Baugh and Sternberg, 2006). Injection of all four genes had the same effect, though injection of *ins-5* had no effect, behaving similar to the negative control with only genetic markers injected. The negative result for *ins-5* is not due to the transmission efficiency of the extrachromosomal array being lower than the others, as evidenced by the fact it also did not affect the relative frequency of transgenic (mCherry-positive) animals among survivors, though *ins-4*, *daf-28* and *ins-6* did (Fig. 7B).

Over-expression of *ins-4*, *ins-6* or *daf-28* also causes an arrest-defective phenotype in starved L1 larvae. The proportion of larvae with at least one M cell division after ten days of L1 starvation was scored. Over-expression of *ins-4* or *daf-28* had the largest average effect on the frequency of larvae with M cell divisions, though *ins-6* over-expression also had a significant effect. Notably, the results for *daf-28* over-expression are only marginally significant ($P=0.06$), but we believe the phenotype is convincing considering how it fits with the other results presented. These results are significant for two reasons. First, they establish an effect of *ins-4*, *daf-28* and *ins-6* on L1 development, though loss-of-function analysis revealed an effect on survival of L1 arrest only. Second, although it is well-established that insulin-like signaling is necessary for L1 development (Baugh and Sternberg, 2006; Fukuyama et al., 2006; Kao et al., 2007), it has not been shown that insulin-like signaling is also sufficient to trigger L1 development.

It is somewhat surprising that over-expression of *ins-6* rescues the *ins-4*; *daf-28* loss-of-function phenotype, reducing starvation survival and even promoting M cell divisions during starvation, since loss of *ins-6* function had no apparent effect. The related role of *ins-6* in regulating dauer exit (Cornils et al., 2011) and its expression in L1 larvae (Fig. 1, Table 1) are consistent with *ins-6* contributing to regulation of L1 arrest and recovery. Nonetheless, over-expression phenotypes must be interpreted cautiously, since they do not necessarily imply that the gene normally functions in that capacity.

Conclusions

This work reveals the temporal and spatial dynamics of insulin-like gene expression during L1 arrest and recovery in *C. elegans*.

We found that expression of the majority of insulin-like genes is influenced by nutrient availability, and we used their expression patterns to classify them as candidate agonists or antagonists of DAF-2/InsR. Meta-analysis of published functional characterizations demonstrates the accuracy of our classifications, revealing substantial correlation between nutrient-dependent regulation of transcription in L1 stage larvae and function as agonist or antagonist throughout the lifecycle. We also found that despite relatively complex expression patterns of the gene family throughout the lifecycle (Pierce et al., 2001; Ritter et al., 2013), candidate agonists are expressed in largely overlapping patterns during L1 arrest and recovery. This spatial expression analysis suggests a role of the chemosensory neurons ASI and ASJ, the interneuron PVT and the intestine in systemic control of L1 development. It also revealed the intestine as the major site of transcriptional control of agonist expression, suggesting that internal nutrient status affects transcription more than sensory perception of the environment.

This work suggests extensive functional overlap among insulin-like genes in nutritional control of L1 development. Comprehensive analysis of insulin-like gene expression during L1 arrest and recovery was used to focus analysis on the best candidates, quantitative assays capable of detecting relatively small phenotypic effects were used, and as many as five candidates were simultaneously disrupted. Nevertheless, cell division and growth rate were not detectably affected by any combination of loss-of-function mutants tested. In contrast, we found that simultaneous loss of *ins-4* and *daf-28* function increases survival of L1 arrest, and over-expression of *ins-4*, *daf-28* or *ins-6* alone decreases survival and causes cell division to occur despite starvation. These results are consistent with their classification as candidate agonists based on expression, but they also underscore the significance of functional redundancy in this context. Redundancy is somewhat expected given the unusually large size of the insulin-like gene family in *C. elegans* (Pierce et al., 2001), but the extent of redundancy is surprising given the relatively specific phenotypic effects of insulin-like genes in other contexts (Cornils et al., 2011; Fernandes de Abreu et al., 2014; Hung et al., 2014; Li et al., 2003; Matsunaga et al., 2012a, 2012b; Michaelson et al., 2010; Murphy et al., 2003).

Nevertheless, there is evidence of functional specificity amidst redundancy. Of ten candidate genes tested, we did uncover phenotypes for three. *ins-4*, *ins-6* and *daf-28* have been implicated in regulation of dauer development (Cornils et al., 2011; Fernandes de Abreu et al., 2014; Hung et al., 2014; Kao et al., 2007; Li et al., 2003; Patel et al., 2008). However, this is the first time these genes have been implicated in regulation of L1 development. Furthermore, the pattern of functional overlap among these three genes in L1 arrest is distinct from dauer development. That is, *ins-6* and *daf-28* mutations have a synergistic effect on dauer formation (Fig. S2), and *ins-4* does not show such an interaction with either (Cornils et al., 2011; Fernandes de Abreu et al., 2014). In contrast, *ins-4* and *daf-28* synergize in regulation of L1 arrest, with *ins-6* apparently contributing in a less significant way. Future work elucidating the mechanistic basis of specificity in insulin-like gene function should explain varying patterns of specificity in different contexts, ultimately addressing why there are so many insulin-like genes in *C. elegans*.

Acknowledgments

We would like to thank Wesley L. Hung and Mei Zhen for sharing the deletion allele *hpDf761* prior to publication. We would like to thank Brad T. Moore for analysis of starvation survival data and Merve Cakir for help with sequence motif analysis. We would also like to thank Nicole Kurhanewicz for technical assistance with mRNA expression analysis and Yi Yin, Brenda Winkler and Emmanuel Mwandosya for generating reporter constructs. Some strains were provided by the CGC, which is funded by NIH Office of Research Infrastructure Programs (P40 OD010440). Additional strains were also provided by Shohei Mitani as part of the National BioResource Project for the Experimental Animal "*Nematode C. elegans*". The Ellison Medical Foundation (New Scholar in Aging Award) and the National Science Foundation (IOS-1120206) supported this work.

Appendix A. Supporting information

Supplementary data associated with this article can be found in the online version at http://dx.doi.org/10.1016/j.ydbio.2014.08.002.

References

Artyukhin, A.B., Schroeder, F.C., Avery, L., 2013. Density dependence in Caenorhabditis larval starvation. Sci. Rep. 3, 2777.
Bailey, T.L., Boden, M., Buske, F.A., Frith, M., Grant, C.E., Clementi, L., Ren, J., Li, W.W., Noble, W.S., 2009. MEME SUITE: tools for motif discovery and searching. Nucleic Acids Res. 37, W202–W208.
Bargmann, C.I., Horvitz, H.R., 1991. Control of larval development by chemosensory neurons in *Caenorhabditis elegans*. Science 251, 1243–1246.
Baugh, L.R., 2009. Staging worms for next-generation analysis. Nat. Methods 6, 727–728.
Baugh, L.R., 2013. To grow or not to grow: nutritional control of development during *Caenorhabditis elegans* L1 Arrest. Genetics 194, 539–555.
Baugh, L.R., Demodena, J., Sternberg, P.W., 2009. RNA Pol II Accumulates at promoters of growth genes during developmental arrest. Science 324 (5923), 92–94.
Baugh, L.R., Kurhanewicz, N., Sternberg, P.W., 2011. Sensitive and precise quantification of insulin-like mRNA expression in *Caenorhabditis elegans*. PloS One 6, e18086.
Baugh, L.R., Sternberg, P.W., 2006. DAF-16/FOXO regulates transcription of cki-1/Cip/Kip and repression of lin-4 during *C. elegans* L1 arrest. Curr. Biol. 16, 780–785.
Cornils, A., Gloeck, M., Chen, Z., Zhang, Y., Alcedo, J., 2011. Specific insulin-like peptides encode sensory information to regulate distinct developmental processes. Development 138, 1183–1193.
Cui, M., Cohen, M.L., Teng, C., Han, M., 2013. The tumor suppressor Rb critically regulates starvation-induced stress response in *C. elegans*. Curr. Biol. 23, 975–980.
Fernandes de Abreu, D.A., Caballero, A., Fardel, P., Stroustrup, N., Chen, Z., Lee, K., Keyes, W.D., Nash, Z.M., Lopez-Moyado, I.F., Vaggi, F., Cornils, A., Regenass, M., Neagu, A., Ostojic, I., Liu, C., Cho, Y., Sifoglu, D., Shen, Y., Fontana, W., Lu, H., Csikasz-Nagy, A., Murphy, C.T., Antebi, A., Blanc, E., Apfeld, J., Zhang, Y., Alcedo, J., Ch'ng, Q., 2014. An insulin-to-insulin regulatory network orchestrates phenotypic specificity in development and physiology. PLoS Genet. 10, e1004225.
Fukuyama, M., Rougvie, A.E., Rothman, J.H., 2006. C. elegans DAF-18/PTEN mediates nutrient-dependent arrest of cell cycle and growth in the germline. Curr. Biol. 16, 773–779.
Geiss, G.K., Bumgarner, R.E., Birditt, B., Dahl, T., Dowidar, N., Dunaway, D.L., Fell, H. P., Ferree, S., George, R.D., Grogan, T., James, J.J., Maysuria, M., Mitton, J.D., Oliveri, P., Osborn, J.L., Peng, T., Ratcliffe, A.L., Webster, P.J., Davidson, E.H., Hood, L., Dimitrov, K., 2008. Direct multiplexed measurement of gene expression with color-coded probe pairs. Nat. Biotechnol. 26, 317–325.
Harfe, B.D., Vaz Gomes, A., Kenyon, C., Liu, J., Krause, M., Fire, A., 1998. Analysis of a *Caenorhabditis elegans* twist homolog identifies conserved and divergent aspects of mesodermal patterning. Genes Dev. 12, 2623–2635.
Hung, W.L., Wang, Y., Chitturi, J., Zhen, M., 2014. A Caenorhabditis elegans developmental decision requires insulin signaling-mediated neuron-intestine communication. Development 141, 1767–1779.
Kao, G., Nordenson, C., Still, M., Ronnlund, A., Tuck, S., Naredi, P., 2007. ASNA-1 positively regulates insulin secretion in *C. elegans* and mammalian cells. Cell 128, 577–587.
Lee, B.H., Ashrafi, K., 2008. A TRPV channel modulates C. elegans neurosecretion, larval starvation survival, and adult lifespan. PLoS Genet. 4, e1000213.
Li, W., Kennedy, S.G., Ruvkun, G., 2003. daf-28 encodes a C. elegans insulin superfamily member that is regulated by environmental cues and acts in the DAF-2 signaling pathway. Genes Dev. 17, 844–858.
Matsunaga, Y., Gengyo-Ando, K., Mitani, S., Iwasaki, T., Kawano, T., 2012a. Physiological function, expression pattern, and transcriptional regulation of a Caenorhabditis elegans insulin-like peptide, INS-18. Biochem. Biophys. Res. Commun. 423, 478–483.
Matsunaga, Y., Nakajima, K., Gengyo-Ando, K., Mitani, S., Iwasaki, T., Kawano, T., 2012b. A Caenorhabditis elegans insulin-like peptide, INS-17: its physiological function and expression pattern. Biosci., Biotechnol. Biochem. 76, 2168–2172.

Maxwell, C.S., Antoshechkin, I., Kurhanewicz, N., Belsky, J.A., Baugh, L.R., 2012. Nutritional control of mRNA isoform expression during developmental arrest and recovery in *C. elegans*. Genome Res. 22, 1920–1929.

Maxwell, C.S., Kruesi, W.S., Core, L.J., Kurhanewicz, N., Waters, C.T., Lewarch, C.L., Antoshechkin, I., Lis, J.T., Meyer, B.J., Baugh, L.R., 2014. Pol II docking and pausing at growth and stress genes in *C. elegans*. Cell Rep..

Michaelson, D., Korta, D.Z., Capua, Y., Hubbard, E.J., 2010. Insulin signaling promotes germline proliferation in C. elegans. Development 137, 671–680.

Moore, B.T., Jordan, J.M., Baugh, L.R., 2013. WormSizer: high-throughput analysis of nematode size and shape. PloS One 8, e57142.

Munoz, M.J., Riddle, D.L., 2003. Positive selection of Caenorhabditis elegans mutants with increased stress resistance and longevity. Genetics 163, 171–180.

Murphy, C.T., Lee, S.J., Kenyon, C., 2007. Tissue entrainment by feedback regulation of insulin gene expression in the endoderm of *Caenorhabditis elegans*. In: Proceedings of the National Academy of Sciences of the United States of America 104, pp. 19046–19050.

Murphy, C.T., McCarroll, S.A., Bargmann, C.I., Fraser, A., Kamath, R.S., Ahringer, J., Li, H., Kenyon, C., 2003. Genes that act downstream of DAF-16 to influence the lifespan of *Caenorhabditis elegans*. Nature 424, 277–283.

Niu, W., Lu, Z.J., Zhong, M., Sarov, M., Murray, J.I., Brdlik, C.M., Janette, J., Chen, C., Alves, P., Preston, E., Slightham, C., Jiang, L., Hyman, A.A., Kim, S.K., Waterston, R.H., Gerstein, M., Snyder, M., Reinke, V., 2011. Diverse transcription factor binding features revealed by genome-wide ChIP-seq in *C. elegans*. Genome Res. 21, 245–254.

Oh, S.W., Mukhopadhyay, A., Dixit, B.L., Raha, T., Green, M.R., Tissenbaum, H.A., 2006. Identification of direct DAF-16 targets controlling longevity, metabolism and diapause by chromatin immunoprecipitation. Nat. Genet. 38, 251–257.

Oliveira, R.P., Porter Abate, J., Dilks, K., Landis, J., Ashraf, J., Murphy, C.T., Blackwell, T.K., 2009. Condition-adapted stress and longevity gene regulation by *Caenorhabditis elegans* SKN-1/Nrf. Aging Cell 8, 524–541.

Patel, D.S., Fang, L.L., Svy, D.K., Ruvkun, G., Li, W., 2008. Genetic identification of HSD-1, a conserved steroidogenic enzyme that directs larval development in *Caenorhabditis elegans*. Development 135, 2239–2249.

Pierce, S.B., Costa, M., Wisotzkey, R., Devadhar, S., Homburger, S.A., Buchman, A.R., Ferguson, K.C., Heller, J., Platt, D.M., Pasquinelli, A.A., Liu, L.X., Doberstein, S.K., Ruvkun, G., 2001. Regulation of DAF-2 receptor signaling by human insulin and ins-1, a member of the unusually large and diverse *C. elegans* insulin gene family. Genes Dev 15, 672–686.

Puig, O., Tjian, R., 2005. Transcriptional feedback control of insulin receptor by dFOXO/FOXO1. Genes Dev. 19, 2435–2446.

Riddle, D.L., Albert, P., 1997. In: elegans II, C., Donald, L., Riddle, T.B., Meyer, Barbara J., Priess, James R. (Eds.), Genetic and Environmental Regulation of Dauer Larva Development in *C. elegans* II. Cold Spring Harbor monograph series. Cold Spring Harbor Laboratory Press, Plainview, N.Y..

Ritter, A.D., Shen, Y., Fuxman Bass, J., Jeyaraj, S., Deplancke, B., Mukhopadhyay, A., Xu, J., Driscoll, M., Tissenbaum, H.A., Walhout, A.J., 2013. Complex expression dynamics and robustness in *C. elegans* insulin networks. Genome Res. 23, 954–965.

Ruaud, A.F., Katic, I., Bessereau, J.L., 2011. Insulin/Insulin-like growth factor signaling controls non-Dauer developmental speed in the nematode *Caenorhabditis elegans*. Genetics 187, 337–343.

Stadler, M., Fire, A., 2013. Conserved translatome remodeling in nematode species executing a shared developmental transition. PLoS Genet. 9, e1003739.

Sulston, J.E., Horvitz, H.R., 1977. Post-embryonic cell lineages of the nematode, *Caenorhabditis elegans*. Dev. Biol. 56, 110–156.

Tepper, R.G., Ashraf, J., Kaletsky, R., Kleemann, G., Murphy, C.T., Bussemaker, H.J., 2013. PQM-1 complements DAF-16 as a key transcriptional regulator of DAF-2-mediated development and longevity. Cell 154, 676–690.

Tullet, J.M., Hertweck, M., An, J.H., Baker, J., Hwang, J.Y., Liu, S., Oliveira, R.P., Baumeister, R., Blackwell, T.K., 2008. Direct inhibition of the longevity-promoting factor SKN-1 by insulin-like signaling in *C. elegans*. Cell 132, 1025–1038.

Vowels, J.J., Thomas, J.H., 1992. Genetic analysis of chemosensory control of dauer formation in *Caenorhabditis elegans*. Genetics 130, 105–123.

Zhong, M., Niu, W., Lu, Z.J., Sarov, M., Murray, J.I., Janette, J., Raha, D., Sheaffer, K.L., Lam, H.Y., Preston, E., Slightham, C., Hillier, L.W., Brock, T., Agarwal, A., Auerbach, R., Hyman, A.A., Gerstein, M., Mango, S.E., Kim, S.K., Waterston, R. H., Reinke, V., Snyder, M., 2010. Genome-wide identification of binding sites defines distinct functions for Caenorhabditis elegans PHA-4/FOXA in development and environmental response. PLoS Genet. 6, e1000848.